



# EFFECTS OF ARRAY SCALING AND ADVANCED BEAMFORMING ON THE ANGULAR RESOLUTION OF MICROPHONE ARRAY SYSTEMS

Matthew Aldeman, Kanthasamy Chelliah, Hirenkumar Patel, and Ganesh Raman  
Illinois Institute of Technology  
10 W. 32<sup>nd</sup> Street, Suite 243, Chicago, IL 60616, USA

## ABSTRACT

Several advanced beamforming methods have been developed in the past 20 years that have dramatically improved the angular resolution of microphone array systems. Meanwhile, the Rayleigh criterion has long been considered the standard criterion for angular resolution of such systems. In this investigation four microphone arrays were constructed as scaled models of a fifth microphone array. All of the arrays were subjected to a thorough regimen of testing with both broadband and narrowband sources. Using conventional beamforming, the angular resolution of each scaled array was determined as a function of frequency and compared to the Rayleigh criterion. The analysis was repeated with the advanced TIDY beamforming algorithm so that the effects of array scaling and advanced beamforming can be determined as a function of frequency and compared to conventional beamforming.

## 1 INTRODUCTION

Microphone array systems have been in use for more than 40 years and have proven useful in a variety of applications [1]. The most traditional form of beamforming is the Delay-and-Sum (DAS) beamforming algorithm, wherein time delays are applied to the pressure signal from each sensor and the resulting signals are summed to form the beamform map [2]. However, the angular resolution of the DAS beamforming algorithm is poor. Frequency-domain beamforming (FDBF) methods were developed in the 1980's using the Fast Fourier Transform. Researchers have since developed improved frequency-domain beamforming algorithms such as CLEAN, RELAX, and SEM. Many such algorithms are based on the idea of manipulating the Cross Spectral Matrix and the concept of spatial source coherence [3,4,5,6,7,8]. More recently, beamforming algorithms have been developed based on methods of deconvolution [9, 10], methods based on the spatial coherence of point sources and sidelobes in the frequency domain [11], and spatial coherence methods in the time domain

[12]. These are the DAMAS, DAMAS2, CLEAN-SC, and TIDY algorithms, respectively. The current investigation will explore the concept of angular resolution utilizing two time-domain beamforming algorithms: the conventional DAS algorithm and the advanced TIDY beamforming algorithm.

The most widely-used criterion for the angular resolution of a microphone array system is the Rayleigh criterion, which indicates that angular resolution is proportional to array diameter and inversely proportional to the signal's wavelength. However, the Rayleigh criterion is a convenient reference point rather than a fixed physical limit. The Rayleigh resolution criterion defines the angular separation between two sources at the point where the Airy disk maximum of one source is located at the first minimum of the second source. The Rayleigh criterion is given by Eq. (1):

$$W = \frac{rD}{\lambda z} \quad (1)$$

where  $r$  is the separation distance between two adjacent sources,  $D$  is the diameter of the array,  $\lambda$  is the wavelength of the sources and  $z$  is the separation distance between the source and the array. The Rayleigh criterion  $W$  is given by the first zero of the first-order Bessel function of the first kind, divided by a factor of pi to convert into radians. This results in a value of  $W = 1.22$ .

The purpose of this work is to experimentally determine the angular resolution of microphone arrays as the array size is scaled to larger and smaller dimensions, and to explore the effect of two beamforming algorithms on the angular resolution of the array. Four microphone arrays have been constructed as scale models of a fifth baseline microphone array. All five arrays have been thoroughly tested, and the results were analyzed first with the conventional DAS algorithm over one-third octave intervals. The results show that the Rayleigh criterion can be exceeded under certain conditions. The same analysis was then performed using the TIDY algorithm on the same data. In this way the effect of array scaling and the effect of the advanced TIDY beamforming method can be determined as a function of frequency and compared to conventional beamforming.

For the experiments carried out in the following sections, a total of four microphone arrays were constructed as scale models of a fifth baseline microphone array. The baseline array has a diameter of 0.73 meters and is hereafter referred to as the "1x" array. An 80% scale model of this array, called the "0.8x" array was constructed with a diameter of 0.59 meters. Scaled-up versions of the baseline array were constructed with diameters that are five, ten, and fifteen times larger than the baseline array. The 5x, 10x, and 15x microphone arrays have diameters of 3.66 meters, 7.32 meters, and 10.98 meters, respectively. Using the Rayleigh criterion, the expected angular resolution is plotted as a function of frequency for each of the five microphone arrays in Fig. 1. The resolvable angular resolution between two acoustic sources (measured in degrees on the horizontal axis) is expected to decrease as either the diameter of the array is increased or the frequency of the signal is increased.

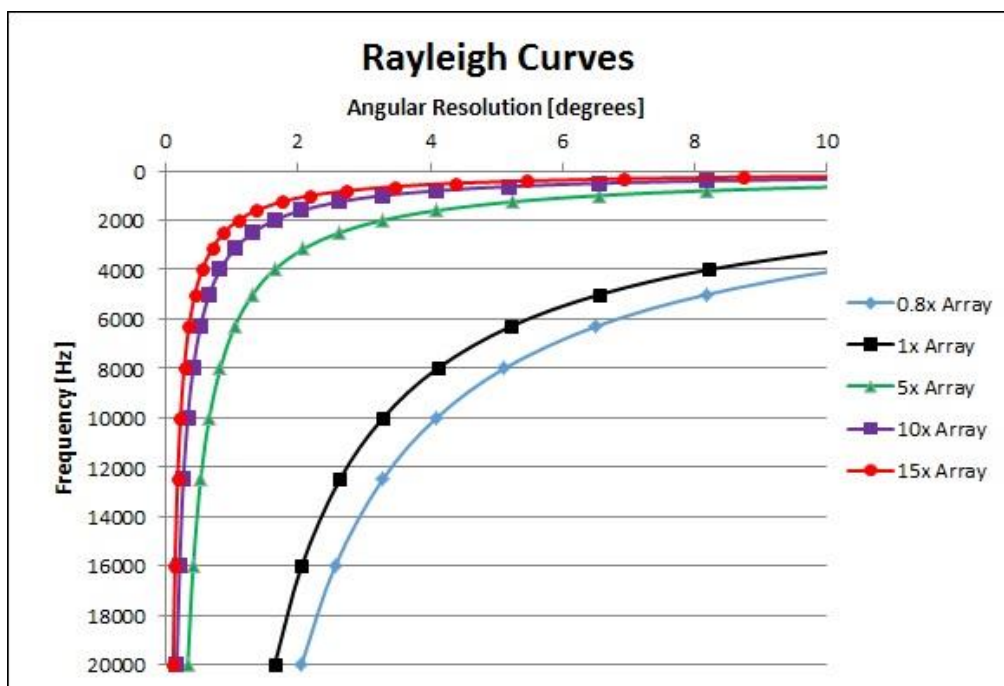


Fig. 1. Expected angular resolution for each of the five microphone arrays.

## 2 FIVE SCALED MICROPHONE ARRAYS

### 2.1 Baseline Array

The baseline array on which each of four scaled microphone arrays are based is the 24-channel OptiNav microphone array produced by OptiNav, Inc. It consists of 24 electret condenser microphones arranged to approximate a multi-arm spiral pattern with a diameter of 0.73 meters. The microphone pressure signals pass through an amplifier and the data is acquired with a MOTU 24 I/O 24-channel chassis. Each channel has 24-bit resolution, and the data is acquired at 44.1 kHz. The MOTU 24 I/O interfaces with a laptop computer equipped with recording software via a PCIe-424 MAGMA Express Box. The data is saved on the laptop for later processing using OptiNav's Beamform Interactive plugin to the ImageJ image processing software. In addition to the microphones, the microphone array contains a video camera in the center of the array. The array's video camera interfaces directly with the laptop computer via USB connection. The OptiNav compact microphone array is shown in Fig. 2.



Fig. 2. OptiNav compact microphone array and data acquisition chassis

## 2.2 Four New Scaled Arrays

For comparison against the baseline OptiNav array, four additional microphone arrays were constructed. The microphone placement within each array is a scaled version of the OptiNav array geometry. The four newly-constructed arrays consist of one scaled-down array with a diameter 80% as large as the OptiNav, and three scaled-up arrays that have diameters of 5, 10, and 15 times greater than the diameter of the OptiNav array. Each array was constructed with 6mm electret condenser microphones, an amplifier circuit with a gain factor of 26, and DB25 parallel-port pinout cards for connection to the same MOTU 24 I/O data acquisition system used by the OptiNav array. The geometry of the array was meticulously laid out. An image of the completed 0.8x array is shown in Fig. 3.



Fig. 3. Completed 0.8x Array

For the scaled-up arrays, a modular construction approach was necessitated by the size of the arrays. Each of the 24 microphones was integrated into a combined breadboard containing the microphone itself and the amplifier circuit. An image of one of the 24 boards is shown in Fig. 4.

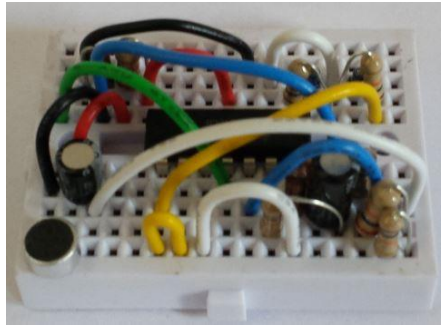


*Fig. 4. Modular breadboard circuit including microphone (lower left) and amplifier circuit*

The array geometry for the 5x, 10x, and 15x arrays was meticulously marked on the roof of a 21-story building at the Illinois Institute of Technology using exterior-grade painters' tape. In this way, the location markings for the microphone circuits were semi-permanently attached, allowing the microphone circuits themselves to be removed when the array was not in use. When they were to be used, the microphone circuit boards were carefully placed in alignment with the tape markings. Images of the fully-assembled 5x, 10x, and 15x arrays are given in Figs. 5, 6, and 7, respectively. In Figs. 6 and 7, the locations of the microphone circuit boards are circled in red for clarity.

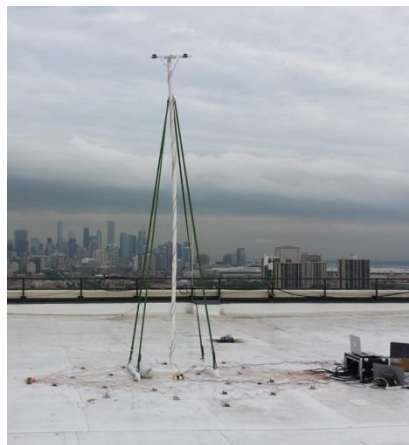


*Fig. 5. 3.66m (5x) Microphone array undergoing testing*

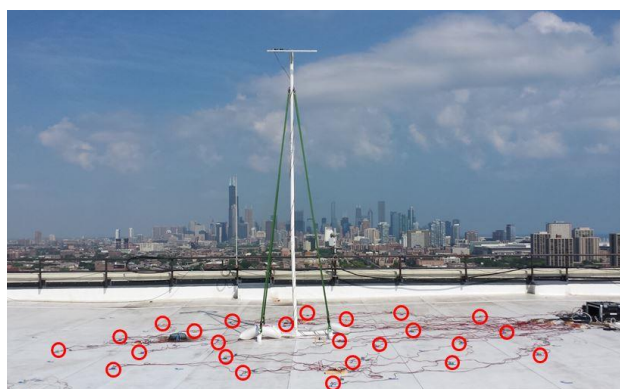


*Fig. 6. 7.32m (10x) Microphone array undergoing testing*

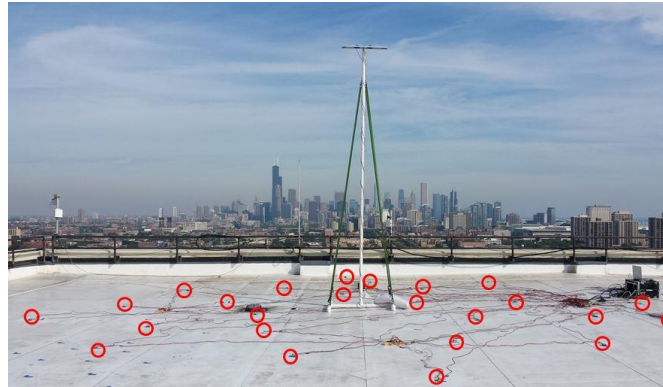


Fig. 7. 10.98m (15x) Microphone array undergoing testing

### 3 ANGULAR RESOLUTION TESTING

Each of the five arrays was subjected to testing at a variety of frequencies, angular separation values, and both broadband and narrowband sources. The test regimen included testing each array at 18 frequencies spaced at one-third octave intervals plus a white noise signal. This sequence was repeated for 19 speaker separation values from 8.9 cm (3.5 in.) to 50.8 cm (20 in.) Thus, the testing sequence involved testing five different microphone arrays at 18 different frequencies for 19 different speaker separation distances. This made a total of 1,710 test cases. The testing regimen is summarized in Table 1.

Table 1. Angular Resolution Testing Regimen

Microphone Array Testing Regimen	
Test Frequencies [Hz]	Speaker Separation [in.]
(200)*	3.5
250	4
315	5
400	6
500	7
630	8
800	9
1,000	10
1,250	11
1,600	12
2,000	13
2,500	14
3,150	15
4,000	16
5,000	17
6,300	18
8,000	19
(10,000)**	20
White Noise	Single Speaker

\* 200 Hz tested on 5x, 10x, and 15x arrays only

\*\* 10,000 Hz tested on 0.8x and 1x arrays only

## 4 RESULTS

The data analysis began by considering the most ubiquitous type of noise source – broadband – and the most conventional of the broadband beamforming algorithms: Delay-and-Sum (DAS). The DAS algorithm has been in use for many decades and serves as a baseline analysis. The DAS algorithm was utilized to construct acoustic source maps for each array, angular separation value, and one-third octave band using the white noise signal. Following analysis, the acoustic source map for each set of conditions was judged to a) consistently resolve the two acoustic sources, b) inconsistently resolve the two acoustic sources, or c) not resolve the two acoustic sources. The second category, where the algorithm inconsistently resolves the two sources, was deemed necessary because there were numerous instances where the algorithm could resolve the sources for certain time steps while it was unable to resolve the sources in all time steps. This typically occurred near the algorithm’s resolution limit for a given array geometry and frequency band. Examples of unresolved, inconsistently resolved, and resolved acoustic sources are given in Fig. 8. The acoustic source maps are overlaid on the image taken with the array video camera. Although the term “inconsistently resolved” refers to inconsistency in the time domain, it is apparent in Fig. 8(b) that the algorithm is very near the resolution limit for this particular set of parameters. Figure 8 shows the results from the 5x array with 25.4 cm (10 in.) of separation between the speakers, corresponding to an angular separation of  $3.1^\circ$ . The differences between Fig. 8(a), 8(b), and 8(c) are due entirely to the frequency band utilized by the DAS algorithm. Figure 8(a) uses a frequency band of 891-1122 Hz, Fig. 8(b) uses a frequency band of 1413-1778 Hz, and Fig. 8(c) utilizes frequencies from 2239-2818 Hz.

The discernment between unresolved, inconsistently resolved, and resolved sources is made more obvious when the acoustic source map is shown by itself against a solid black background rather than overlaid over an image. Figure 9 shows the same acoustic source maps without the image of the test apparatus.

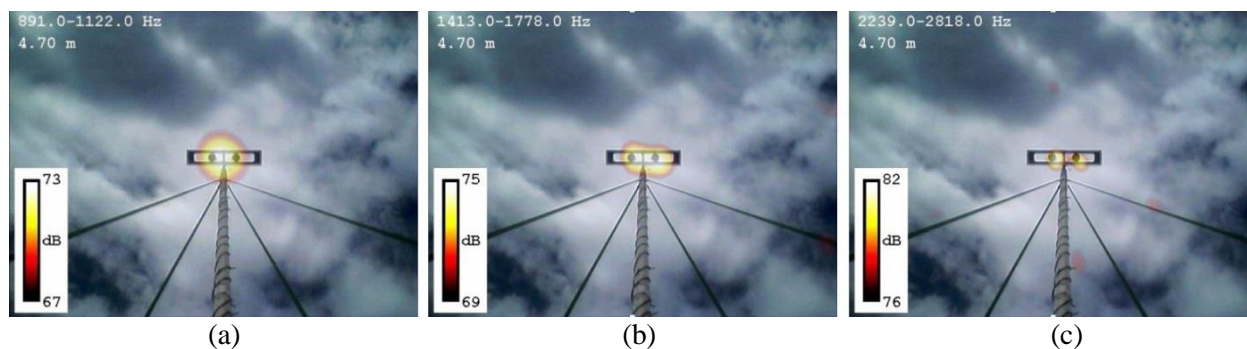


Fig. 8. (a) Unresolved, (b) Inconsistently Resolved, and (c) Resolved noise sources

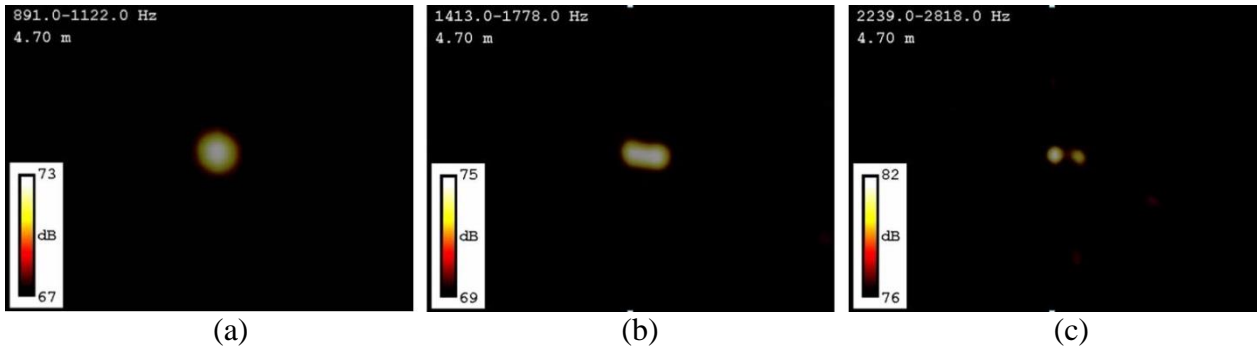


Fig. 9. (a) Unresolved, (b) Inconsistently Resolved, and (c) Resolved noise sources without images

### 4.1 DAS Results

This analysis was carried out using the DAS algorithm for each array, each frequency band, and each speaker separation distance. The results for the five arrays are given in Tables 2 through 6. In each case, the discretized Rayleigh criterion curve is plotted as “R”s along with the results. Where the algorithm consistently resolves the two sources, the bin is colored green. Where the algorithm inconsistently resolves the sources the bin is colored yellow, and where the algorithm cannot resolve the sources the bin is colored red.

Table 2. DAS Angular Resolution Results for 0.8x Array

Array: 0.8x	Speaker Separation [in.]																					
	3.5	4	5	6	7	8	9	10	11	12	13	14	15	16	17	18	19	20				
	Angular Separation [°]																					
Freq. band [Hz]	1.62	1.85	2.31	2.77	3.23	3.69	4.16	4.62	5.08	5.54	6.00	6.46	6.92	7.38	7.84	8.30	8.76	9.22				
178-224	R																					
224-282	R																					
282-355	R																					
355-447	R																					
447-562	R																					
562-708	R																					
708-891	R																					
891-1122	R																					
1122-1413	R																					
1413-1778	R																					
1778-2239	R																					
2239-2818	R														Y		Y					
2818-3548	R										Y			G		G						
3548-4467	R										Y		G		G		G		G		R	
4467-5623	R				Y		G		G		G		G		G		G		R			
5623-7079	R				Y		G		G		G		G		G		G		R			
7079-8913	R				Y		G		G		G		G		G		G		R			
8913-11220	R				Y		G		G		G		G		G		G		R			
11220-14130	R		Y		G		G		G		G		G		G		G		R			
14130-17780	R		Y		G		G		G		G		G		G		G		R			
17780-22390	R		Y		G		G		G		G		G		G		G		R			

Table 3. DAS Angular Resolution Results for 1x Array

Array: 1x	Speaker Separation [in.]																			
	3.5	4	5	6	7	8	9	10	11	12	13	14	15	16	17	18	19	20		
Freq. band [Hz]	Angular Separation [°]																			
	1.62	1.85	2.31	2.77	3.23	3.69	4.16	4.62	5.08	5.54	6.00	6.46	6.92	7.38	7.84	8.30	8.76	9.22		
178-224	Red	Red	Red	Red	Red	Red	Red	Red	Red	Red	Red	Red	Red	Red	Red	Red	Red	Red	Red	
224-282	Red	Red	Red	Red	Red	Red	Red	Red	Red	Red	Red	Red	Red	Red	Red	Red	Red	Red	Red	
282-355	Red	Red	Red	Red	Red	Red	Red	Red	Red	Red	Red	Red	Red	Red	Red	Red	Red	Red	Red	
355-447	Red	Red	Red	Red	Red	Red	Red	Red	Red	Red	Red	Red	Red	Red	Red	Red	Red	Red	Red	
447-562	Red	Red	Red	Red	Red	Red	Red	Red	Red	Red	Red	Red	Red	Red	Red	Red	Red	Red	Red	
562-708	Red	Red	Red	Red	Red	Red	Red	Red	Red	Red	Red	Red	Red	Red	Red	Red	Red	Red	Red	
708-891	Red	Red	Red	Red	Red	Red	Red	Red	Red	Red	Red	Red	Red	Red	Red	Red	Red	Red	Red	
891-1122	Red	Red	Red	Red	Red	Red	Red	Red	Red	Red	Red	Red	Red	Red	Red	Red	Red	Red	Red	
1122-1413	Red	Red	Red	Red	Red	Red	Red	Red	Red	Red	Red	Red	Red	Red	Red	Red	Red	Red	Red	
1413-1778	Red	Red	Red	Red	Red	Red	Red	Red	Red	Red	Red	Red	Red	Red	Red	Red	Red	Red	Red	
1778-2239	Red	Red	Red	Red	Red	Red	Red	Red	Red	Red	Red	Red	Red	Red	Red	Red	Red	Red	Red	
2239-2818	Red	Red	Red	Red	Red	Red	Red	Red	Red	Red	Red	Red	Red	Red	Red	Red	Red	Red	Red	
2818-3548	Red	Red	Red	Red	Red	Red	Red	Red	Red	Red	Red	Red	Red	Red	Red	Red	Red	Red	Red	
3548-4467	Red	Red	Red	Red	Red	Red	Red	Red	Red	Red	Red	Red	Red	Red	Red	Red	Red	Red	Red	
4467-5623	Red	Red	Red	Red	Red	Red	Red	Red	Red	Red	Red	Red	Red	Red	Red	Red	Red	Red	Red	
5623-7079	Red	Red	Red	Red	Red	Red	Red	Red	Red	Red	Red	Red	Red	Red	Red	Red	Red	Red	Red	
7079-8913	Red	Red	Red	Red	Red	Red	Red	Red	Red	Red	Red	Red	Red	Red	Red	Red	Red	Red	Red	
8913-11220	Red	Red	Red	Red	Red	Red	Red	Red	Red	Red	Red	Red	Red	Red	Red	Red	Red	Red	Red	
11220-14130	Red	Red	Red	Red	Red	Red	Red	Red	Red	Red	Red	Red	Red	Red	Red	Red	Red	Red	Red	
14130-17780	Red	Red	Red	Red	Red	Red	Red	Red	Red	Red	Red	Red	Red	Red	Red	Red	Red	Red	Red	
17780-22390	Red	Red	Red	Red	Red	Red	Red	Red	Red	Red	Red	Red	Red	Red	Red	Red	Red	Red	Red	

Table 4. DAS Angular Resolution Results for 5x Array

Array: 5x	Speaker Separation [in.]																			
	3.5	4	5	6	7	8	9	10	11	12	13	14	15	16	17	18	19	20		
Freq. band [Hz]	Angular Separation [°]																			
	1.08	1.24	1.55	1.86	2.17	2.48	2.79	3.10	3.41	3.71	4.02	4.33	4.64	4.95	5.26	5.57	5.88	6.19		
178-224	Red	Red	Red	Red	Red	Red	Red	Red	Red	Red	Red	Red	Red	Red	Red	Red	Red	Red	Red	
224-282	Red	Red	Red	Red	Red	Red	Red	Red	Red	Red	Red	Red	Red	Red	Red	Red	Red	Red	Red	
282-355	Red	Red	Red	Red	Red	Red	Red	Red	Red	Red	Red	Red	Red	Red	Red	Red	Red	Red	Red	
355-447	Red	Red	Red	Red	Red	Red	Red	Red	Red	Red	Red	Red	Red	Red	Red	Red	Red	Red	Red	
447-562	Red	Red	Red	Red	Red	Red	Red	Red	Red	Red	Red	Red	Red	Red	Red	Red	Red	Red	Red	
562-708	Red	Red	Red	Red	Red	Red	Red	Red	Red	Red	Red	Red	Red	Red	Red	Red	Red	Red	Red	
708-891	Red	Red	Red	Red	Red	Red	Red	Red	Red	Red	Red	Red	Red	Red	Red	Red	Red	Red	Red	
891-1122	Red	Red	Red	Red	Red	Red	Red	Red	Red	Red	Red	Red	Red	Red	Red	Red	Red	Red	Red	
1122-1413	Red	Red	Red	Red	Red	Red	Red	Red	Red	Red	Red	Red	Red	Red	Red	Red	Red	Red	Red	
1413-1778	Red	Red	Red	Red	Red	Red	Red	Red	Red	Red	Red	Red	Red	Red	Red	Red	Red	Red	Red	
1778-2239	Red	Red	Red	Red	Red	Red	Red	Red	Red	Red	Red	Red	Red	Red	Red	Red	Red	Red	Red	
2239-2818	Red	Red	Red	Red	Red	Red	Red	Red	Red	Red	Red	Red	Red	Red	Red	Red	Red	Red	Red	
2818-3548	Red	Red	Red	Red	Red	Red	Red	Red	Red	Red	Red	Red	Red	Red	Red	Red	Red	Red	Red	
3548-4467	Red	Red	Red	Red	Red	Red	Red	Red	Red	Red	Red	Red	Red	Red	Red	Red	Red	Red	Red	
4467-5623	Red	Red	Red	Red	Red	Red	Red	Red	Red	Red	Red	Red	Red	Red	Red	Red	Red	Red	Red	
5623-7079	Red	Red	Red	Red	Red	Red	Red	Red	Red	Red	Red	Red	Red	Red	Red	Red	Red	Red	Red	
7079-8913	Red	Red	Red	Red	Red	Red	Red	Red	Red	Red	Red	Red	Red	Red	Red	Red	Red	Red	Red	
8913-11220	Red	Red	Red	Red	Red	Red	Red	Red	Red	Red	Red	Red	Red	Red	Red	Red	Red	Red	Red	
11220-14130	Red	Red	Red	Red	Red	Red	Red	Red	Red	Red	Red	Red	Red	Red	Red	Red	Red	Red	Red	
14130-17780	Red	Red	Red	Red	Red	Red	Red	Red	Red	Red	Red	Red	Red	Red	Red	Red	Red	Red	Red	
17780-22390	Red	Red	Red	Red	Red	Red	Red	Red	Red	Red	Red	Red	Red	Red	Red	Red	Red	Red	Red	

Table 5. DAS Angular Resolution Results for 10x Array

Array: 10x	Speaker Separation [in.]																			
	3.5	4	5	6	7	8	9	10	11	12	13	14	15	16	17	18	19	20		
	Angular Separation [°]																			
Freq. band [Hz]	1.08	1.24	1.55	1.86	2.17	2.48	2.79	3.10	3.41	3.71	4.02	4.33	4.64	4.95	5.26	5.57	5.88	6.19		
178-224	Red																			
224-282	Red																			
282-355	Red																			
355-447	Red																			
447-562	Red																			
562-708	Red																			
708-891	Red																			
891-1122	Red																			
1122-1413	Red																			
1413-1778	Red																			
1778-2239	Red																			
2239-2818	Red																			
2818-3548	Red																			
3548-4467	Red																			
4467-5623	Red																			
5623-7079	Red																			
7079-8913	Red																			
8913-11220	Red																			
11220-14130	Red																			
14130-17780	Red																			
17780-22390	Red																			

Table 6. DAS Angular Resolution Results for 15x Array

Array: 15x	Speaker Separation [in.]																			
	3.5	4	5	6	7	8	9	10	11	12	13	14	15	16	17	18	19	20		
	Angular Separation [°]																			
Freq. band [Hz]	1.08	1.24	1.55	1.86	2.17	2.48	2.79	3.10	3.41	3.71	4.02	4.33	4.64	4.95	5.26	5.57	5.88	6.19		
178-224	Red																			
224-282	Red																			
282-355	Red																			
355-447	Red																			
447-562	Red																			
562-708	Red																			
708-891	Red																			
891-1122	Red																			
1122-1413	Red																			
1413-1778	Red																			
1778-2239	Red																			
2239-2818	Red																			
2818-3548	Red																			
3548-4467	Red																			
4467-5623	Red																			
5623-7079	Red																			
7079-8913	Red																			
8913-11220	Red																			
11220-14130	Red																			
14130-17780	Red																			
17780-22390	Red																			

The lower operating frequency limit of the arrays, denoted in Tables 2-6 by the uppermost green and yellow bins, is limited by the ability of the algorithm to resolve two acoustic sources at low frequencies. It is apparent that the Rayleigh criterion can indeed be exceeded under certain conditions. It appears that the Rayleigh limit becomes increasingly difficult to exceed as the array size increases, even though the calculation of the Rayleigh limit already incorporates the array diameter. This could possibly be due to a source of error discussed in Section 4.4.

The upper operating frequency limit, denoted in Tables 2-6 by the lowermost green and yellow bins, is limited by the appearance and subsequent dominance of grating lobes. As the frequency increases, the inter-element spacing becomes larger relative to the wavelength, which will eventually lead to grating lobes. At the upper frequency limit, the actual acoustic sources in the acoustic source map are no longer distinguishable from the grating lobes. Because each array in this experiment has an identical number of microphones, the inter-element spacing becomes larger as the array size increases. Thus, the useful upper frequency limit is reduced as the array size is increased.

### 4.2 TIDY Results

The analysis described above was repeated using the TIDY beamforming algorithm. The TIDY algorithm is an advanced time-domain beamforming algorithm useful for improved beamforming of broadband sources. The results are given below in Tables 7 through 11.

Table 7. TIDY Angular Resolution Results for 0.8x Array

Array: 0.8x	Speaker Separation [in.]																			
	3.5	4	5	6	7	8	9	10	11	12	13	14	15	16	17	18	19	20		
	Angular Separation [°]																			
Freq. band [Hz]	1.62	1.85	2.31	2.77	3.23	3.69	4.16	4.62	5.08	5.54	6.00	6.46	6.92	7.38	7.84	8.30	8.76	9.22		
178-224	Red	Red	Red	Red	Red	Red	Red	Red	Red	Red	Red	Red	Red	Red	Red	Red	Red	Red	Red	
224-282	Red	Red	Red	Red	Red	Red	Red	Red	Red	Red	Red	Red	Red	Red	Red	Red	Red	Red	Red	
282-355	Red	Red	Red	Red	Red	Red	Red	Red	Red	Red	Red	Red	Red	Red	Red	Red	Red	Red	Red	
355-447	Red	Red	Red	Red	Red	Red	Red	Red	Red	Red	Red	Red	Red	Red	Red	Red	Red	Red	Red	
447-562	Red	Red	Red	Red	Red	Red	Red	Red	Red	Red	Red	Red	Red	Red	Red	Red	Red	Red	Red	
562-708	Red	Red	Red	Red	Red	Red	Red	Red	Red	Red	Red	Red	Red	Red	Red	Red	Red	Red	Red	
708-891	Red	Red	Red	Red	Red	Red	Red	Red	Red	Red	Red	Red	Red	Red	Red	Red	Red	Red	Red	
891-1122	Red	Red	Red	Red	Red	Red	Red	Red	Red	Red	Red	Red	Red	Red	Red	Red	Red	Red	Red	
1122-1413	Red	Red	Red	Red	Red	Red	Red	Red	Red	Red	Red	Red	Red	Red	Red	Red	Red	Red	Red	
1413-1778	Red	Red	Red	Red	Red	Red	Red	Red	Red	Red	Red	Red	Red	Red	Red	Red	Red	Red	Red	
1778-2239	Red	Red	Red	Red	Red	Red	Red	Red	Red	Red	Red	Red	Red	Red	Red	Red	Red	Red	Red	
2239-2818	Red	Red	Red	Red	Red	Red	Red	Red	Red	Red	Red	Red	Red	Red	Red	Red	Red	Red	Red	
2818-3548	Red	Red	Red	Red	Red	Red	Red	Red	Red	Red	Red	Red	Red	Red	Red	Red	Red	Red	Red	
3548-4467	Red	Red	Red	Red	Red	Red	Red	Red	Red	Red	Red	Red	Red	Red	Red	Red	Red	Red	Red	
4467-5623	Red	Red	Red	Red	Red	Red	Red	Red	Red	Red	Red	Red	Red	Red	Red	Red	Red	Red	Red	
5623-7079	Red	Red	Red	Red	Red	Red	Red	Red	Red	Red	Red	Red	Red	Red	Red	Red	Red	Red	Red	
7079-8913	Red	Red	Red	Red	Red	Red	Red	Red	Red	Red	Red	Red	Red	Red	Red	Red	Red	Red	Red	
8913-11220	Red	Red	Red	Red	Red	Red	Red	Red	Red	Red	Red	Red	Red	Red	Red	Red	Red	Red	Red	
11220-14130	Red	Red	Red	Red	Red	Red	Red	Red	Red	Red	Red	Red	Red	Red	Red	Red	Red	Red	Red	
14130-17780	Red	Red	Red	Red	Red	Red	Red	Red	Red	Red	Red	Red	Red	Red	Red	Red	Red	Red	Red	
17780-22390	Red	Red	Red	Red	Red	Red	Red	Red	Red	Red	Red	Red	Red	Red	Red	Red	Red	Red	Red	

Table 8. TIDY Angular Resolution Results for 1x Array

Array: 1x	Speaker Separation [in.]																			
	3.5	4	5	6	7	8	9	10	11	12	13	14	15	16	17	18	19	20		
	Angular Separation [°]																			
Freq. band [Hz]	1.62	1.85	2.31	2.77	3.23	3.69	4.16	4.62	5.08	5.54	6.00	6.46	6.92	7.38	7.84	8.30	8.76	9.22		
178-224	Red	Red	Red	Red	Red	Red	Red	Red	Red	Red	Red	Red	Red	Red	Red	Red	Red	Red	Red	
224-282	Red	Red	Red	Red	Red	Red	Red	Red	Red	Red	Red	Red	Red	Red	Red	Red	Red	Red	Red	
282-355	Red	Red	Red	Red	Red	Red	Red	Red	Red	Red	Red	Red	Red	Red	Red	Red	Red	Red	Red	
355-447	Red	Red	Red	Red	Red	Red	Red	Red	Red	Red	Red	Red	Red	Red	Red	Red	Red	Red	Red	
447-562	Red	Red	Red	Red	Red	Red	Red	Red	Red	Red	Red	Red	Red	Red	Red	Red	Red	Red	Red	
562-708	Red	Red	Red	Red	Red	Red	Red	Red	Red	Red	Red	Red	Red	Red	Red	Red	Red	Red	Red	
708-891	Red	Red	Red	Red	Red	Red	Red	Red	Red	Red	Red	Red	Red	Red	Red	Red	Red	Red	Red	
891-1122	Red	Red	Red	Red	Red	Red	Red	Red	Red	Red	Red	Red	Red	Red	Red	Red	Red	Red	Red	
1122-1413	Red	Red	Red	Red	Red	Red	Red	Red	Red	Red	Red	Red	Red	Red	Red	Red	Red	Red	Red	
1413-1778	Red	Red	Red	Red	Red	Red	Red	Red	Red	Red	Red	Red	Red	Red	Red	Red	Red	Red	Red	
1778-2239	Red	Red	Red	Red	Red	Red	Red	Red	Red	Red	Red	Red	Red	Red	Red	Red	Red	Red	Yellow	
2239-2818	Red	Red	Red	Red	Red	Red	Red	Red	Red	Red	Red	Red	Red	Red	Red	Red	Red	Red	Green	
2818-3548	Red	Red	Red	Red	Red	Red	Red	Red	Red	Red	Red	Red	Red	Red	Red	Red	Red	Red	Green	
3548-4467	Red	Red	Red	Red	Red	Red	Red	Red	Red	Red	Red	Red	Red	Red	Red	Red	Red	Red	Green	
4467-5623	Red	Red	Red	Red	Red	Red	Red	Red	Red	Red	Red	Red	Red	Red	Red	Red	Red	Red	Green	
5623-7079	Red	Red	Red	Red	Red	Red	Red	Red	Red	Red	Red	Red	Red	Red	Red	Red	Red	Red	Green	
7079-8913	Red	Red	Red	Red	Red	Red	Red	Red	Red	Red	Red	Red	Red	Red	Red	Red	Red	Red	Green	
8913-11220	Red	Red	Red	Red	Red	Red	Red	Red	Red	Red	Red	Red	Red	Red	Red	Red	Red	Red	Green	
11220-14130	Red	Red	Red	Red	Red	Red	Red	Red	Red	Red	Red	Red	Red	Red	Red	Red	Red	Red	Green	
14130-17780	Red	Red	Red	Red	Red	Red	Red	Red	Red	Red	Red	Red	Red	Red	Red	Red	Red	Red	Green	
17780-22390	Red	Red	Red	Red	Red	Red	Red	Red	Red	Red	Red	Red	Red	Red	Red	Red	Red	Red	Green	

Table 9. TIDY Angular Resolution Results for 5x Array

Array: 5x	Speaker Separation [in.]																			
	3.5	4	5	6	7	8	9	10	11	12	13	14	15	16	17	18	19	20		
	Angular Separation [°]																			
Freq. band [Hz]	1.08	1.24	1.55	1.86	2.17	2.48	2.79	3.10	3.41	3.71	4.02	4.33	4.64	4.95	5.26	5.57	5.88	6.19		
178-224	Red	Red	Red	Red	Red	Red	Red	Red	Red	Red	Red	Red	Red	Red	Red	Red	Red	Red	Red	
224-282	Red	Red	Red	Red	Red	Red	Red	Red	Red	Red	Red	Red	Red	Red	Red	Red	Red	Red	Red	
282-355	Red	Red	Red	Red	Red	Red	Red	Red	Red	Red	Red	Red	Red	Red	Red	Red	Red	Red	Red	
355-447	Red	Red	Red	Red	Red	Red	Red	Red	Red	Red	Red	Red	Red	Red	Red	Red	Red	Red	Red	
447-562	Red	Red	Red	Red	Red	Red	Red	Red	Red	Red	Red	Red	Red	Red	Red	Red	Red	Red	Red	
562-708	Red	Red	Red	Red	Red	Red	Red	Red	Red	Red	Red	Red	Red	Red	Red	Red	Red	Red	Red	
708-891	Red	Red	Red	Red	Red	Red	Red	Red	Red	Red	Red	Red	Red	Red	Red	Red	Red	Red	Red	
891-1122	Red	Red	Red	Red	Red	Red	Red	Red	Red	Red	Red	Red	Red	Red	Red	Red	Red	Red	Red	
1122-1413	Red	Red	Red	Red	Red	Red	Red	Red	Red	Red	Red	Red	Red	Red	Red	Red	Red	Red	Red	
1413-1778	Red	Red	Red	Red	Red	Red	Red	Red	Red	Red	Red	Red	Red	Red	Red	Red	Red	Red	Red	
1778-2239	Red	Red	Red	Red	Red	Red	Red	Red	Red	Red	Red	Red	Red	Red	Red	Red	Red	Red	Red	
2239-2818	Red	Red	Red	Red	Red	Red	Red	Red	Red	Red	Red	Red	Red	Red	Red	Red	Red	Red	Red	
2818-3548	Red	Red	Red	Red	Red	Red	Red	Red	Red	Red	Red	Red	Red	Red	Red	Red	Red	Red	Red	
3548-4467	Red	Red	Red	Red	Red	Red	Red	Red	Red	Red	Red	Red	Red	Red	Red	Red	Red	Red	Red	
4467-5623	Red	Red	Red	Red	Red	Red	Red	Red	Red	Red	Red	Red	Red	Red	Red	Red	Red	Red	Red	
5623-7079	Red	Red	Red	Red	Red	Red	Red	Red	Red	Red	Red	Red	Red	Red	Red	Red	Red	Red	Red	
7079-8913	Red	Red	Red	Red	Red	Red	Red	Red	Red	Red	Red	Red	Red	Red	Red	Red	Red	Red	Red	
8913-11220	Red	Red	Red	Red	Red	Red	Red	Red	Red	Red	Red	Red	Red	Red	Red	Red	Red	Red	Red	
11220-14130	Red	Red	Red	Red	Red	Red	Red	Red	Red	Red	Red	Red	Red	Red	Red	Red	Red	Red	Red	
14130-17780	Red	Red	Red	Red	Red	Red	Red	Red	Red	Red	Red	Red	Red	Red	Red	Red	Red	Red	Red	
17780-22390	Red	Red	Red	Red	Red	Red	Red	Red	Red	Red	Red	Red	Red	Red	Red	Red	Red	Red	Red	

Table 10. TIDY Angular Resolution Results for 10x Array

Array: 10x	Speaker Separation [in.]																			
	3.5	4	5	6	7	8	9	10	11	12	13	14	15	16	17	18	19	20		
Freq. band [Hz]	Angular Separation [°]																			
	1.08	1.24	1.55	1.86	2.17	2.48	2.79	3.10	3.41	3.71	4.02	4.33	4.64	4.95	5.26	5.57	5.88	6.19		
178-224	Red	Red	Red	Red	Red	Red	Red	Red	Red	Red	Red	Red	Red	Red	Red	Red	Red	Red	Red	
224-282	Red	Red	Red	Red	Red	Red	Red	Red	Red	Red	Red	Red	Red	Red	Red	Red	Red	Red	Red	
282-355	Red	Red	Red	Red	Red	Red	Red	Red	Red	Red	Red	Red	Red	Red	Red	Red	Red	Red	Red	
355-447	Red	Red	Red	Red	Red	Red	Red	Red	Red	Red	Red	Red	Red	Red	Red	Red	Red	Red	Red	
447-562	Red	Red	Red	Red	Red	Red	Red	Red	Red	Red	Red	Red	Red	Red	Red	Red	Red	Red	Red	
562-708	Red	Red	Red	Red	Red	Red	Red	Red	Red	Red	Red	Red	Red	Red	Red	Red	Red	Red	Red	
708-891	Red	Red	Red	Red	Red	Red	Red	Red	Red	Red	Red	Red	Red	Red	Red	Red	Red	Red	Red	
891-1122	Red	Red	Red	Red	Red	Red	Red	Red	Red	Red	Red	Red	Red	Red	Red	Red	Red	Red	Red	
1122-1413	Red	Red	Red	Red	Red	Red	Red	Red	Red	Red	Red	Red	Red	Red	Red	Red	Red	Red	Red	
1413-1778	Red	Red	Red	Red	Red	Red	Red	Red	Red	Red	Red	Red	Red	Red	Red	Red	Red	Red	Red	
1778-2239	Red	Red	Red	Red	Red	Red	Red	Red	Red	Red	Red	Red	Red	Red	Red	Red	Red	Red	Red	
2239-2818	Red	Red	Red	Red	Red	Red	Red	Red	Red	Red	Red	Red	Red	Red	Red	Red	Red	Red	Red	
2818-3548	Red	Red	Red	Red	Red	Red	Red	Red	Red	Red	Red	Red	Red	Red	Red	Red	Red	Red	Red	
3548-4467	Red	Red	Red	Red	Red	Red	Red	Red	Red	Red	Red	Red	Red	Red	Red	Red	Red	Red	Red	
4467-5623	Red	Red	Red	Red	Red	Red	Red	Red	Red	Red	Red	Red	Red	Red	Red	Red	Red	Red	Red	
5623-7079	Red	Red	Red	Red	Red	Red	Red	Red	Red	Red	Red	Red	Red	Red	Red	Red	Red	Red	Red	
7079-8913	Red	Red	Red	Red	Red	Red	Red	Red	Red	Red	Red	Red	Red	Red	Red	Red	Red	Red	Red	
8913-11220	Red	Red	Red	Red	Red	Red	Red	Red	Red	Red	Red	Red	Red	Red	Red	Red	Red	Red	Red	
11220-14130	Red	Red	Red	Red	Red	Red	Red	Red	Red	Red	Red	Red	Red	Red	Red	Red	Red	Red	Red	
14130-17780	Red	Red	Red	Red	Red	Red	Red	Red	Red	Red	Red	Red	Red	Red	Red	Red	Red	Red	Red	
17780-22390	Red	Red	Red	Red	Red	Red	Red	Red	Red	Red	Red	Red	Red	Red	Red	Red	Red	Red	Red	

Table 11. TIDY Angular Resolution Results for 15x Array

Array: 15x	Speaker Separation [in.]																			
	3.5	4	5	6	7	8	9	10	11	12	13	14	15	16	17	18	19	20		
Freq. band [Hz]	Angular Separation [°]																			
	1.08	1.24	1.55	1.86	2.17	2.48	2.79	3.10	3.41	3.71	4.02	4.33	4.64	4.95	5.26	5.57	5.88	6.19		
178-224	Red	Red	Red	Red	Red	Red	Red	Red	Red	Red	Red	Red	Red	Red	Red	Red	Red	Red	Red	
224-282	Red	Red	Red	Red	Red	Red	Red	Red	Red	Red	Red	Red	Red	Red	Red	Red	Red	Red	Red	
282-355	Red	Red	Red	Red	Red	Red	Red	Red	Red	Red	Red	Red	Red	Red	Red	Red	Red	Red	Red	
355-447	Red	Red	Red	Red	Red	Red	Red	Red	Red	Red	Red	Red	Red	Red	Red	Red	Red	Red	Red	
447-562	Red	Red	Red	Red	Red	Red	Red	Red	Red	Red	Red	Red	Red	Red	Red	Red	Red	Red	Red	
562-708	Red	Red	Red	Red	Red	Red	Red	Red	Red	Red	Red	Red	Red	Red	Red	Red	Red	Red	Red	
708-891	Red	Red	Red	Red	Red	Red	Red	Red	Red	Red	Red	Red	Red	Red	Red	Red	Red	Red	Red	
891-1122	Red	Red	Red	Red	Red	Red	Red	Red	Red	Red	Red	Red	Red	Red	Red	Red	Red	Red	Red	
1122-1413	Red	Red	Red	Red	Red	Red	Red	Red	Red	Red	Red	Red	Red	Red	Red	Red	Red	Red	Red	
1413-1778	Red	Red	Red	Red	Red	Red	Red	Red	Red	Red	Red	Red	Red	Red	Red	Red	Red	Red	Red	
1778-2239	Red	Red	Red	Red	Red	Red	Red	Red	Red	Red	Red	Red	Red	Red	Red	Red	Red	Red	Red	
2239-2818	Red	Red	Red	Red	Red	Red	Red	Red	Red	Red	Red	Red	Red	Red	Red	Red	Red	Red	Red	
2818-3548	Red	Red	Red	Red	Red	Red	Red	Red	Red	Red	Red	Red	Red	Red	Red	Red	Red	Red	Red	
3548-4467	Red	Red	Red	Red	Red	Red	Red	Red	Red	Red	Red	Red	Red	Red	Red	Red	Red	Red	Red	
4467-5623	Red	Red	Red	Red	Red	Red	Red	Red	Red	Red	Red	Red	Red	Red	Red	Red	Red	Red	Red	
5623-7079	Red	Red	Red	Red	Red	Red	Red	Red	Red	Red	Red	Red	Red	Red	Red	Red	Red	Red	Red	
7079-8913	Red	Red	Red	Red	Red	Red	Red	Red	Red	Red	Red	Red	Red	Red	Red	Red	Red	Red	Red	
8913-11220	Red	Red	Red	Red	Red	Red	Red	Red	Red	Red	Red	Red	Red	Red	Red	Red	Red	Red	Red	
11220-14130	Red	Red	Red	Red	Red	Red	Red	Red	Red	Red	Red	Red	Red	Red	Red	Red	Red	Red	Red	
14130-17780	Red	Red	Red	Red	Red	Red	Red	Red	Red	Red	Red	Red	Red	Red	Red	Red	Red	Red	Red	
17780-22390	Red	Red	Red	Red	Red	Red	Red	Red	Red	Red	Red	Red	Red	Red	Red	Red	Red	Red	Red	

Compared to the DAS results in Tables 2-6 the TIDY results show both superior angular resolution at low frequencies and superior mitigation of grating lobes at high frequencies. This results in an expanded operating range for the TIDY algorithm as compared to the DAS algorithm, which appears as an expanded green region in the results tables above. Each one of the arrays shows a significant increase in performance with the TIDY algorithm as compared to the DAS algorithm. However, the smaller arrays (0.8x, 1x, 5x) exhibit particularly large gains in performance, with the gains occurring at both the low and high frequency edges of the useful operating region.

As the size of the array increased, the angular resolution performance of the array improved in absolute terms. That is, for a given frequency, a larger array consistently resolved the sources at a smaller separation angle. However, as the array size increased the angular resolution performance of the array tended to decrease relative to the Rayleigh criterion. The 0.8x array greatly exceeded the Rayleigh criterion over its entire useful operating region, while the performance of the 1x array relative to the Rayleigh criterion was only slightly lower. The 5x array consistently outperformed the Rayleigh criterion over its operating range, but its performance relative to the Rayleigh criterion was slightly lower. The 10x array consistently met the Rayleigh criterion over the higher-frequency portion of its operating range, but as the frequency decreased the 10x array was not able to consistently meet the Rayleigh criterion. However, the 10x array was able to inconsistently match the Rayleigh criterion over most of the low-frequency portion of its operating range. Finally, the 15x array came close to meeting the Rayleigh criterion over the high-frequency portion of its range, but was not able to meet the Rayleigh criterion – even on an inconsistent basis – at the lowest frequencies. The cause of this relative decrease in performance is not immediately clear, but several possible explanations are explored in Section 4.4.

When the array size increased, the effective upper frequency limit decreased. This is expected, and is due to the increasing inter-element spacing as the array size grows larger. Larger inter-element spacing results in the onset and subsequent dominance of grating lobes at lower frequencies because the spacing becomes larger relative to the signal wavelength. The exception to this pattern was between the 0.8x array and the 1x array, where the 1x array had a higher upper frequency limit than the 0.8x array. This was probably due to the manufacturing precision of the 1x array as compared to the 0.8x array. The 1x array was built by OptiNav using precision machining of sheet metal. The 0.8x array was built by the author out of oak plywood, and while extreme care was taken in order to be as precise as possible, the placement of the microphones is probably not as precise as the OptiNav array. At very high frequencies, small microphone placement errors may lead to decreased performance.

### 4.3 Angular Resolution Comparison by Array Size and Algorithm

A summary of each array's angular resolution performance can be seen by plotting the minimum consistently resolvable angular separation for each array at each frequency band. This type of plot facilitates a simple comparison of angular resolution between arrays. Fig. 10 shows the minimum consistently resolvable angular separation for each array using the DAS algorithm, and Fig. 11 shows the minimum consistently resolvable angular separation for each array using the TIDY algorithm.

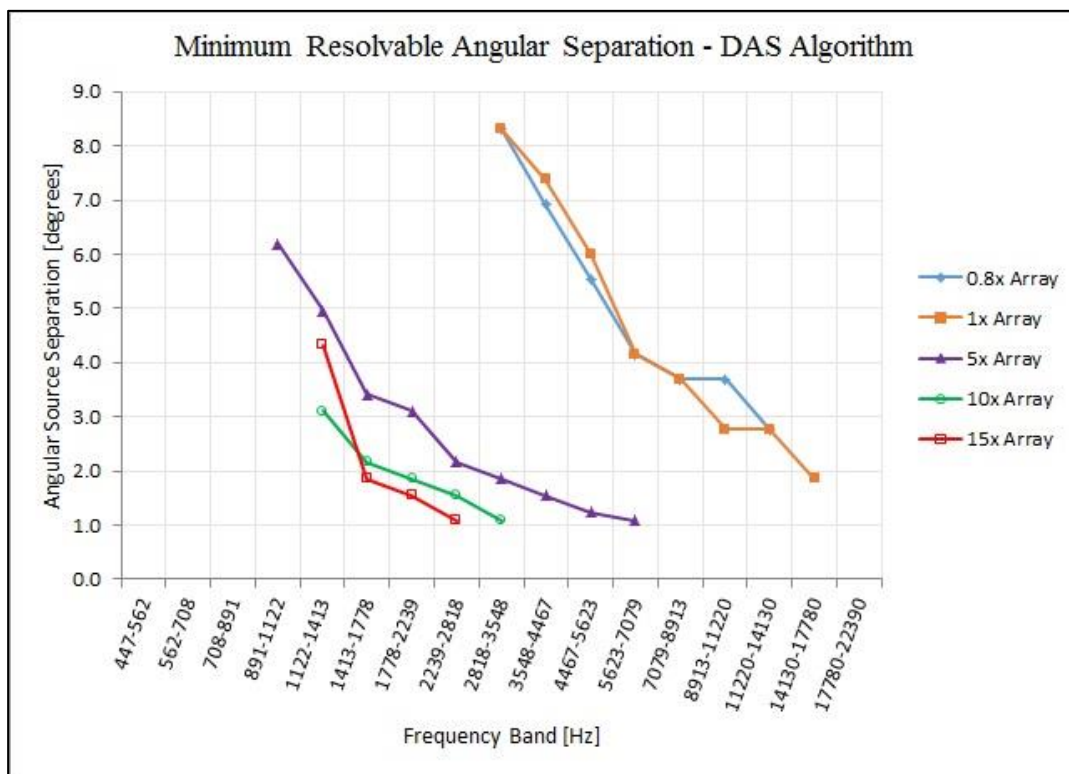


Fig. 10. Minimum Angular Resolution Data for 0.8x, 1x, 5x, 10x, and 15x arrays using DAS algorithm

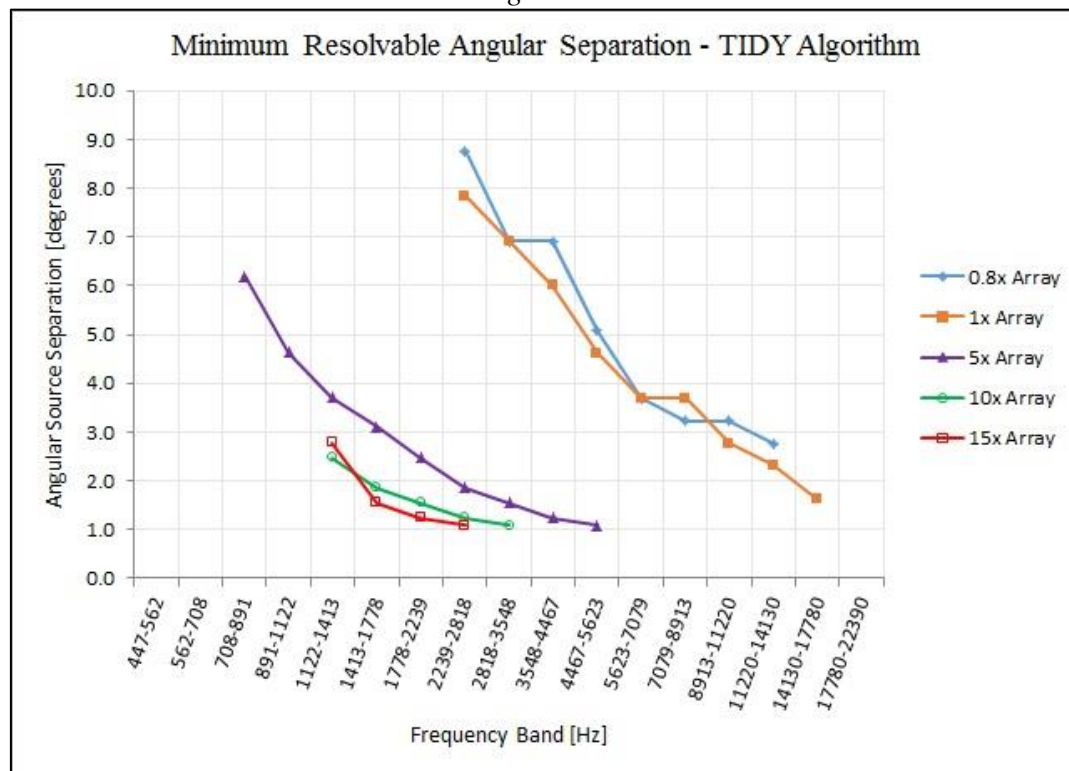


Fig. 11. Minimum Angular Resolution Data for 0.8x, 1x, 5x, 10x, and 15x arrays using TIDY algorithm

Several observations can be made from inspection of Figs. 10 and 11. First, the minimum resolvable separation almost always decreases when the array size increased, as expected. Second, the arrays clearly have different operating bands. Thus, a different array may be selected for an application depending on the frequency of the expected signal. Finally, comparison of the DAS and TIDY plots shows that the TIDY algorithm provides superior angular resolution. For a given array, the angular resolution curve in the TIDY plot is generally shifted down (to smaller angular separation values) and/or shifted left (to lower frequencies) as compared to the DAS plot.

Another useful metric is the performance of each array and each algorithm as compared to the Rayleigh criterion. As discussed in Sections 4.1 and 4.2, some combinations of arrays and algorithms greatly exceed the Rayleigh criterion, while some do not meet the Rayleigh criterion at all. For the purpose of comparison between arrays, the angular separation required for resolution in each case can be normalized by the angular separation suggested by the Rayleigh criterion in each case. A system that greatly exceeds the Rayleigh criterion will have an angular separation required for resolution that is much smaller than the separation angle suggested by the Rayleigh criterion. Thus, its normalized performance will be less than one. A system that does not meet the Rayleigh criterion will have a required angular separation for resolution that is greater than the separation angle suggested by the Rayleigh criterion, and will therefore have a normalized performance that is greater than one. This metric is calculated and plotted for each array and each algorithm at each frequency band, and the result is shown in Fig. 12.

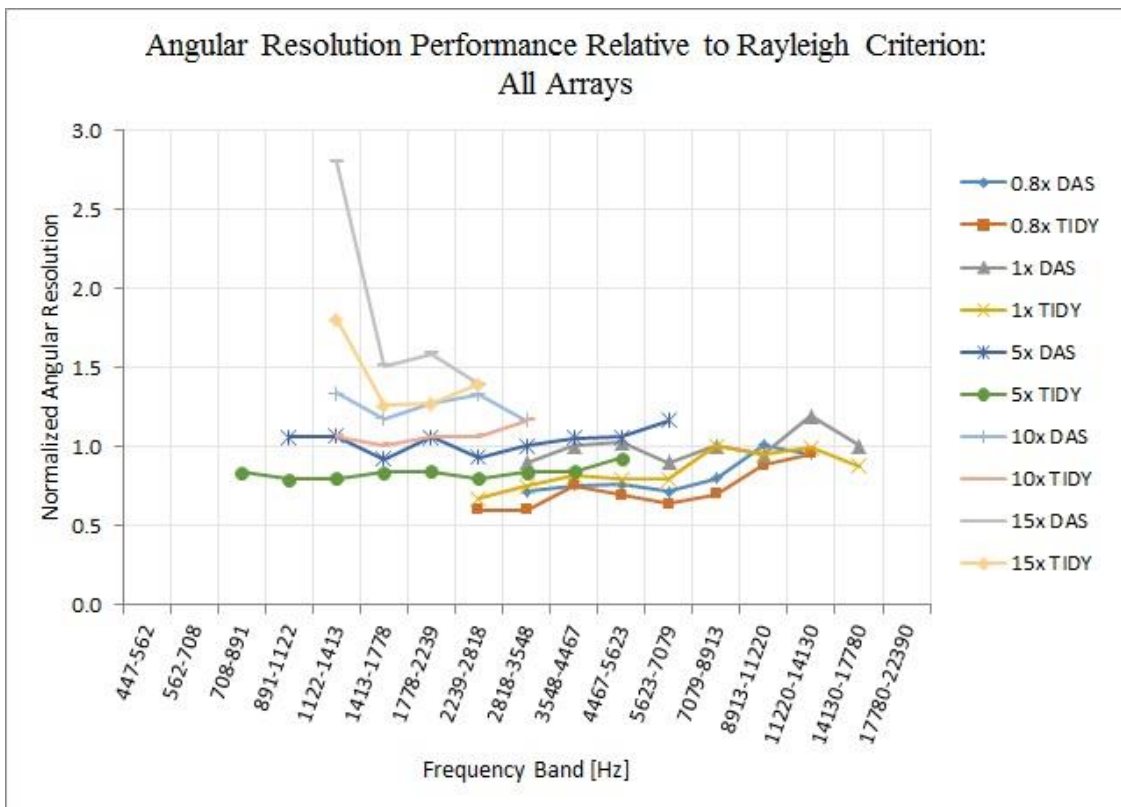


Fig. 12. Normalized performance of each array and each algorithm at each frequency band

The lower curves in Fig. 12 represent the best angular resolution performance relative to the Rayleigh criterion. In general, Fig. 12 shows that the smaller arrays tend to outperform the large arrays relative to the Rayleigh criterion, and that the TIDY algorithm tends to outperform DAS. Thus, the lower curves in Fig. 12 (representing the best performance relative to the Rayleigh criterion) are dominated by the smaller arrays and the TIDY algorithm, while the upper curves generally represent the larger arrays and the DAS algorithm.

#### 4.4 Addressing Potential Sources of Error

The DAS and TIDY results presented in the previous sections exhibit profiles that approximate the shape of the Rayleigh curve. However, the relative performance of the arrays compared to each other is not thoroughly explained by the Rayleigh criterion alone. For example, the smaller 0.8x and 1x arrays easily outperform the Rayleigh criterion by significant margins. Meanwhile, the larger 10x and 15x arrays are only barely capable of meeting the Rayleigh criterion, and in some cases cannot meet the Rayleigh criterion. There are several possible reasons for this:

- i. **Signal-to-Noise Ratio (SNR):** It is possible that the larger arrays – especially at the outside edges – are suffering from poor SNR. This may reduce the effective diameter of the array, thereby reducing the low-frequency performance.
- ii. **Z-axis correction:** The initial testing and analysis described above was performed with the assumption that the rooftop under the arrays is a perfectly flat horizontal plane. Accurately measuring and re-analyzing the data with corrected z-axis measurements may improve the results.
- iii. **Signal reflection effects:** The arrays are assumed to be operating in a free field environment, but of course this is not entirely accurate. The roof has a concrete safety barrier approximately 1 meter tall extending around the perimeter of the roof. As the array size increases, the microphones must be positioned closer to the barrier. Reflection of the test signal off the concrete perimeter barrier may adversely affect the performance of the larger arrays.

##### *Signal-to-Noise Ratio (SNR) Effects*

Potential SNR issues could be adversely affecting the output of the larger arrays. The SNR may be acceptable for the smaller arrays because they are closer to the acoustic test sources. But as the radius of the array increases and the array elements become farther away from the test sources, the SNR could decrease. This could reduce the effective diameter of the larger arrays, which would impair the ability of the array to resolve sources at low frequencies. Fortunately, there is a relatively simple test to check if poor SNR is affecting the beamforming output. To check for SNR impacts, the integration time for the beamforming map can be varied. If SNR is adversely affecting the output, then the results will improve with longer integration times. If SNR is not significantly affecting the output, then the beamforming results will vary little as the integration time is changed. This check was performed for both DAS and TIDY algorithms across several different angular separation distances and for different initial beamforming results (i.e. green, yellow, and red cells in Tables 2-11). For brevity, only one such example case will be given here. Because it may

offer the best chance to show improvement, a marginal or “yellow” (inconsistently resolved) case will be shown below. The inconsistently resolved case for the 15x array at 20.3cm (8 in.) speaker separation with the DAS algorithm at 1122-1413 Hz is given in Fig. 13.

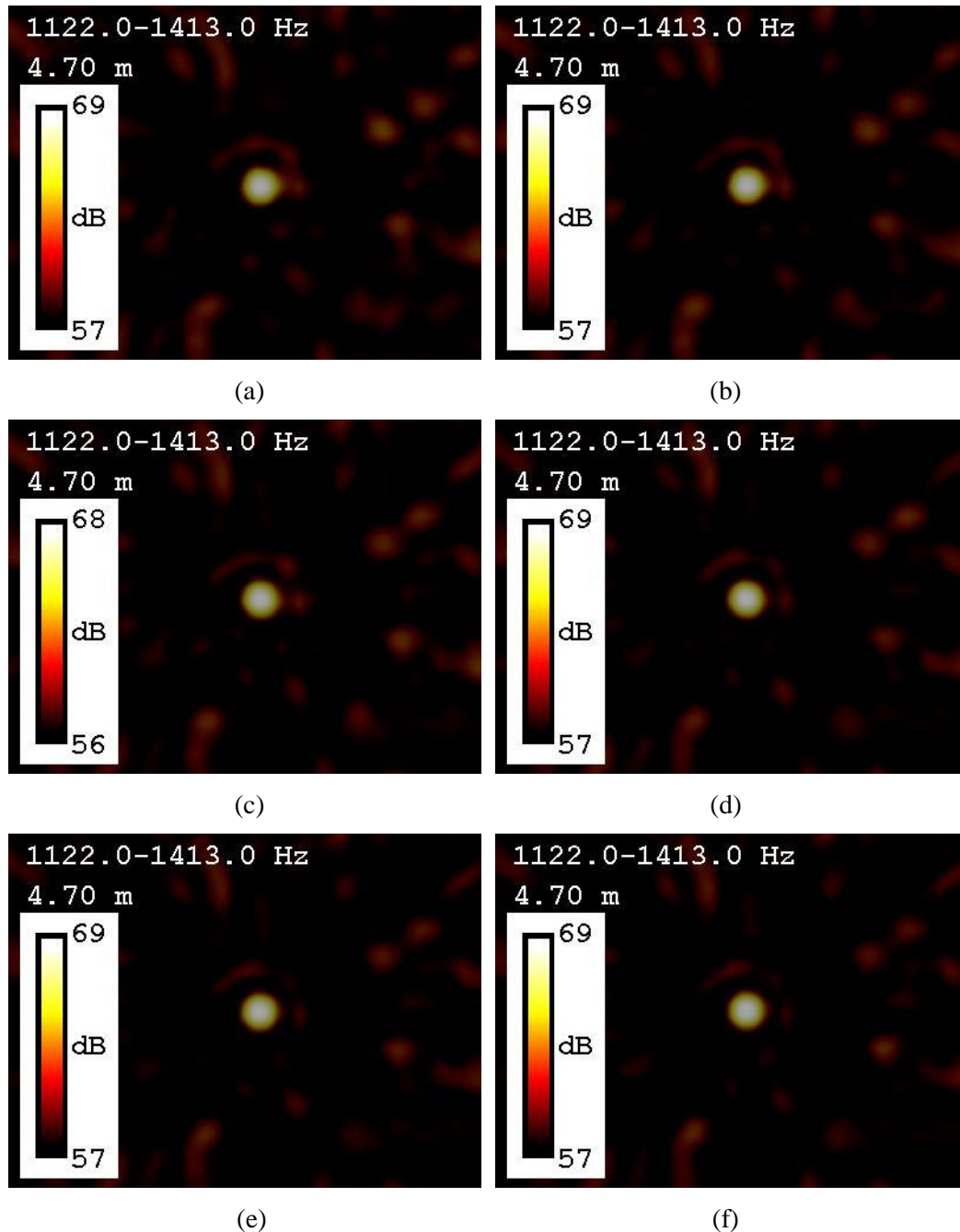


Fig. 13. Beamforming map for 15x array at 20.3cm (8in.) speaker separation with DAS algorithm at 1122-1413 Hz using integration times of (a) 0.1s, (b) 0.2s, (c) 0.4s, (d) 0.8s, (e) 2.0s, and (f) 4.0s.

As can be seen in Fig. 13, the beamforming map does not significantly change as the integration time is varied from 0.1s to 4.0s. This effect is consistent across both algorithms, all source separation distances, and regardless of initial beamforming result. This indicates that the SNR is not significantly affecting the beamforming output.

### *Z-axis Correction*

When the 5x, 10x and 15x microphone arrays were laid out on the rooftop, it was assumed that the roof was a flat horizontal plane. Even if this is not true, the error was assumed to be small. However, errors in z position could be affecting the results. To address this potential issue, z-axis measurements were taken and the results were re-analyzed with the corrected microphone position geometry.

To measure the z-axis position of the microphone array elements, a rotary laser level was placed at the center of each array and leveled. A measuring stick was then placed at every microphone position, and the height of the laser level plane above the microphone position was recorded. By subtracting the average z measurement from each individual measurement, the z-axis coordinate of each microphone was obtained. The average magnitude (absolute value) of the z correction for individual elements in the 5x array was 1.0 cm (0.41 in.), while for the 10x and 15x arrays the average magnitude of the z corrections were 2.8 cm (1.12 in.) and 3.3 cm (1.31 in.), respectively. The array geometry was updated with the corrected z-axis coordinates and the beamforming analysis was re-performed for each case. For brevity the full results tables are not shown here, but the effects are discussed below.

The z-axis correction could potentially impact the beamforming results in two distinct ways. It could impact the arrays' ability to resolve low frequency sources, i.e. it may affect the angular resolution performance relative to the Rayleigh criterion. Alternatively or additionally, the correction may impact the upper frequency limit of the array, i.e. the maximum frequency at which the array can effectively operate before the onset and dominance of grating lobes. Each of these possibilities will be tested separately.

The effect of z-axis correction on the performance of the array relative to the Rayleigh criterion will be discussed first. To show this potential effect, the minimum frequency at which the beamforming map was able to consistently resolve sources at each angular separation distance was recorded. This is analogous to the upper-most green cell in each column of Tables 2-11. This may be considered the "angular resolution frontier." It is the curve representing the lowest frequency at which the algorithm can consistently resolve two acoustic sources at a given angular separation. The angular resolution frontier curves for uncorrected and z-corrected analysis of each array are presented in Fig. 14 (DAS) and Fig. 15 (TIDY). The data for the 0.8x and 1x arrays is not shown because the microphones on the smaller arrays were installed on a flat plate rather than the rooftop. Therefore there is no z correction for the 0.8x and 1x arrays.

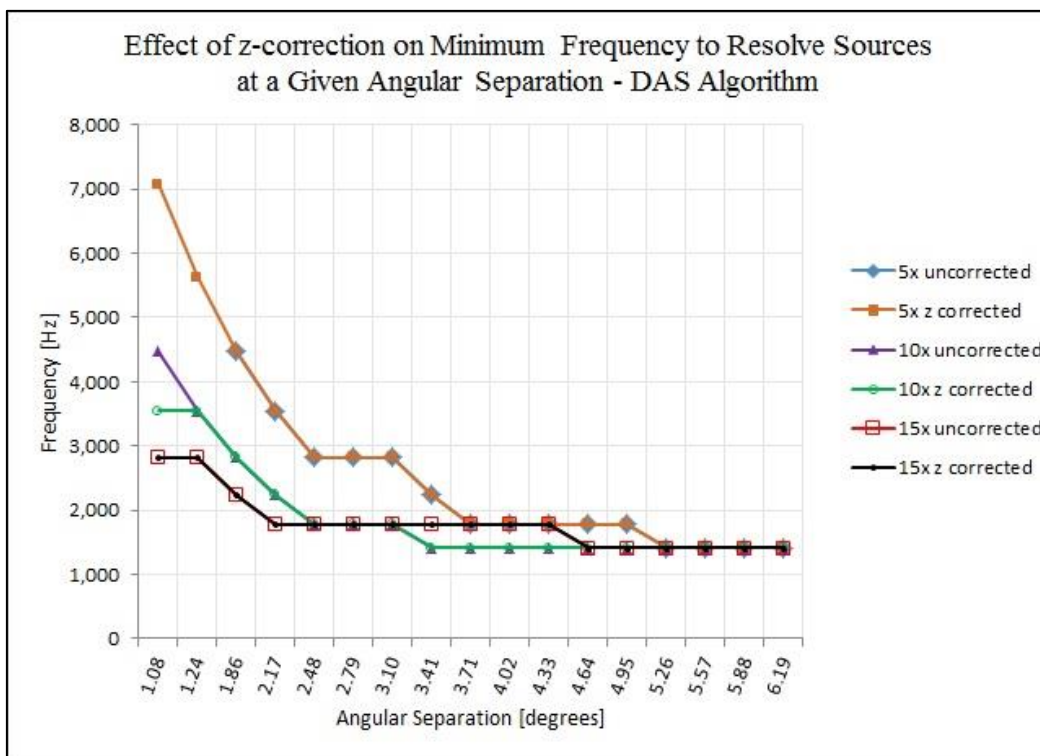


Fig. 14. Angular resolution frontier curve for uncorrected and z-corrected analysis of 5x, 10x, and 15x arrays with the DAS algorithm

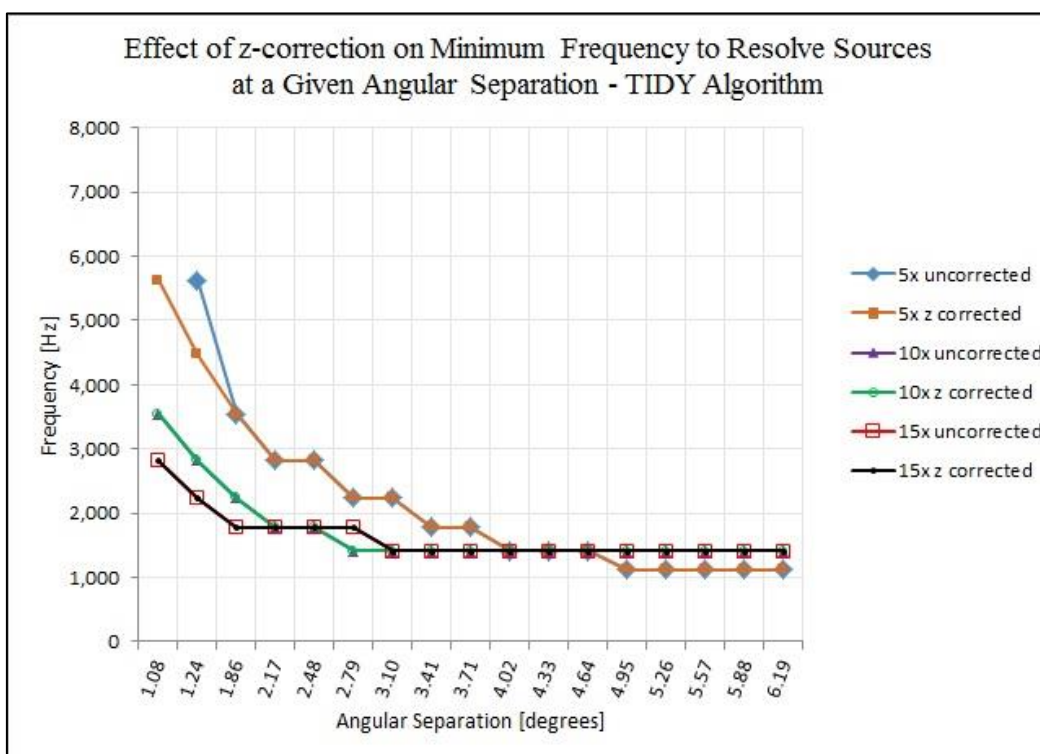


Fig. 15. Angular resolution frontier curve for uncorrected and z-corrected analysis of 5x, 10x, and 15x arrays with the TIDY algorithm.

A number of conclusions can be drawn from inspection of Figs. 14 and 15. First, it is apparent that for a given angular separation, the TIDY algorithm is able to achieve resolution at a lower frequency band than the DAS algorithm. This is consistent with earlier discussion in Sections 4.2 and 4.3. Second, it is also apparent that a larger array is usually able to achieve resolution for a given angular separation at a lower frequency band than a smaller array. Finally, it can be seen that the uncorrected and z-corrected curves for a particular array generally lie on top of each other. That is, the uncorrected and z-corrected angular resolution frontier curves are nearly identical. This means that the z-axis correction did not significantly impact the angular resolution performance of the arrays relative to the Rayleigh criterion. This is logical, as the signal wavelengths in this region are on the order of 10-35 cm while the average z errors are on the order of 1-3 cm. Therefore, the data and the plots in Section 4.3 remain essentially unchanged.

The effect of z-axis correction on the upper frequency limit of the array will be analyzed next. The upper frequency limit is the maximum frequency that the beamforming system can achieve before grating lobes dominate the beamform map. In contrast to the low-frequency resolution, the upper frequency limit of the array does not depend on angular separation of the sources. This can be seen in Tables 2-11, where the bottom edge of the green region is a roughly horizontal line segment. Because it does not depend on angular separation of the sources, an average can be taken across all angular separation values for each array and algorithm. By averaging the maximum frequency achieved by each array and each algorithm with both uncorrected and z-corrected geometries, the effect of z correction on the upper frequency limit can be determined. The average upper frequency limits are shown in Fig. 16 (DAS) and Fig. 17 (TIDY).

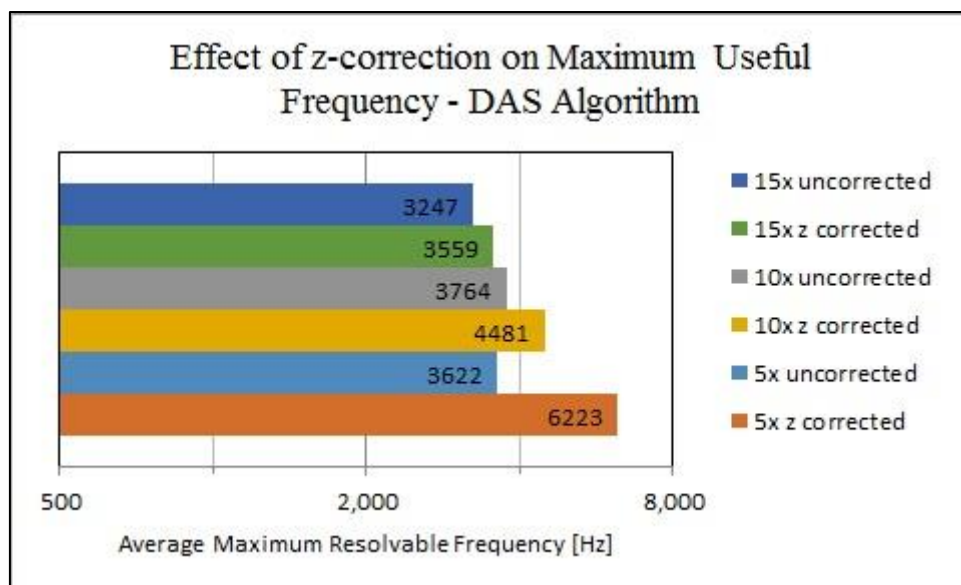


Fig. 16. Average Maximum Frequency for uncorrected and z-corrected geometry with 5x, 10x, and 15x arrays using DAS algorithm

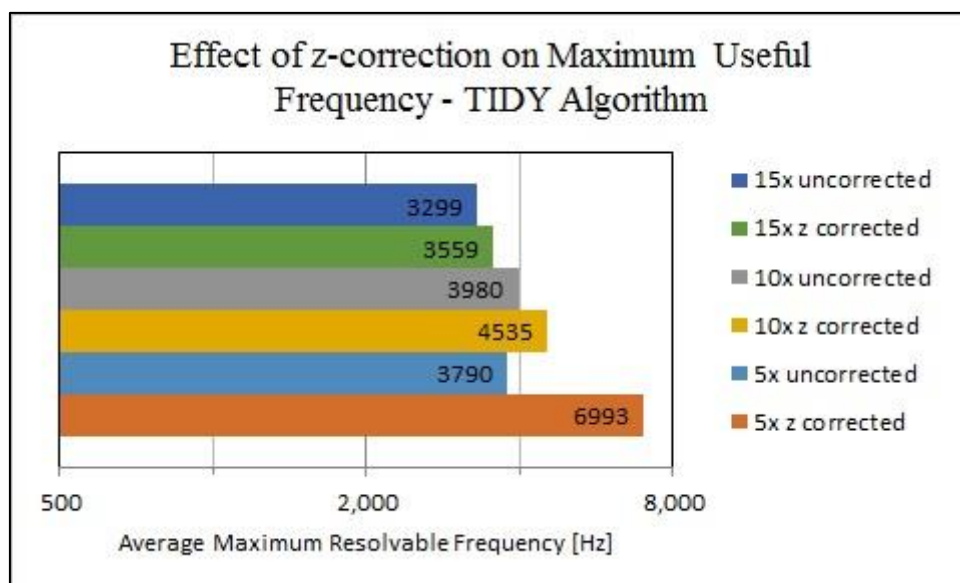


Fig. 17. Average Maximum Frequency for uncorrected and z-corrected geometry with 5x, 10x, and 15x arrays using TIDY algorithm

By inspection of Figs. 16 and 17 it is apparent that z-coordinate correction has a significant impact on the upper frequency limit. In every case, z correction improved the upper frequency limit of the array system. The effect was most pronounced with the 5x array. This is likely because the smaller inter-element spacing of the 5x array meant that it had greater potential to operate at higher frequencies, but it could not do so without precise microphone placement geometry. Even the 15x array showed significant improvement, although it showed less improvement than the 5x and 10x arrays. This is likely because the larger inter-element spacing of the 15x array means that it is not capable of operating at very high frequencies even with very precise microphone placement.

#### Signal Reflection Effects at Boundaries

Another potential source of error is the possibility of signal reflection effects at boundaries near the edge of the larger arrays. The arrays are assumed to be operating in a free field environment, but of course this is not entirely accurate. In addition to various ventilation equipment located on the rooftop, the roof has a concrete safety barrier approximately 1 meter tall extending around the perimeter of the roof. As the array size increases, the microphones must be located closer to the concrete barrier. In the largest (15x) array, the closest microphone is located approximately one meter from the wall. Reflection of the test signal off the concrete perimeter barrier may adversely affect the performance of the larger arrays.

To test this hypothesis, an experiment will be conducted in a controlled laboratory environment. Several array geometries will be laid out on a horizontal surface in an open laboratory environment approximating a free field. A complete battery of angular resolution testing will be performed using the same test apparatus that was used to test the arrays on the roof. Next, a barrier will be constructed around the perimeter of the array. The angular resolution testing will be repeated. The results from these test conditions will be compared,

and the comparison will provide empirical insight into the effect of perimeter boundary reflection.

## 5 SUMMARY

A series of experiments was conducted to determine the operating characteristics of five scaled microphone arrays. It is apparent from the tables of results that each array has a different operating range in terms of frequency and angular resolution. This reinforces the fact that the important performance characteristics of an array must be specified at an early stage of development so that the important parameters of the array can be designed accordingly. For increased angular resolution, the array should have a large diameter and/or it should operate at high frequencies. To increase the upper frequency limit of the useful operating range, the inter-element spacing should be kept small compared to the wavelength of interest.

The results of these experiments show the angular resolution of each array using the DAS beamforming algorithm as well as the TIDY algorithm compared against the Rayleigh criterion curve. TIDY is shown to outperform the DAS algorithm in nearly every case. In some cases, especially with smaller arrays using the TIDY algorithm, the Rayleigh criterion can be significantly exceeded. In other cases, especially with larger arrays and the DAS algorithm, it is very difficult to achieve resolution meeting the Rayleigh criterion. The next step will be to perform the same angular resolution analysis using several other advanced beamforming algorithms such as DAMAS, DAMAS2 and CLEAN-SC. In addition, an experiment will be performed in a controlled laboratory environment to explore the effect of perimeter boundary reflection on the angular resolution of microphone arrays.

## REFERENCES

- [1] Michel, U. "History of Acoustic Beamforming." Berlin Beamforming Conference, Berlin. 2006.
- [2] Johnson, D.H. & Dudgeon, D.E. *Array Signal Processing: Concepts and Techniques*. Prentice Hall. 1993.
- [3] R.P. Dougherty, R.W. Stoker. "Sidelobe suppression for phased array aeroacoustic measurements." American Institute of Aeronautics and Astronautics Paper 98-2242. 1998.
- [4] R.P. Dougherty. "Beamforming in Acoustic Testing", in T.J. Mueller (ed.) *Aeroacoustic Measurements*. Springer. New York. 2002.
- [5] S. Oerlemans, P. Sijtsma. "Determination of Absolute Levels from Phased Array Measurements using Spatial Source Coherence." American Institute of Aeronautics and Astronautics Paper 2002-2464. 2002.
- [6] T.F. Brooks, W.M. Humphreys Jr. "Flap Edge Aeroacoustic Measurements and Predictions." *J. Sound Vib.* 261, 31-74. 2003.

- [7] Y. Wang, J. Li, P. Stoica, M. Sheplak, T. Nishida. "Wideband RELAX and wideband CLEAN for aeroacoustic imaging." American Institute of Aeronautics and Astronautics Paper 2003-3197. 2003.
- [8] D. Blacodon, G. Elias. "Level Estimation of Extended Acoustic Sources using an Array of Microphones." American Institute of Aeronautics and Astronautics Paper 2003-3199. 2003.
- [9] T.F. Brooks and W.M. Humphreys, Jr. "A Deconvolution Approach for the Mapping of Acoustic Sources (DAMAS) determined from phased microphone array." J. Sound Vib. 294 (4-5), 856-879. 2006.
- [10] R.P. Dougherty. "Extensions of DAMAS and Benefits and Limitations of Deconvolution in Beamforming." American Institute of Aeronautics and Astronautics Paper 2005-2961. 2005.
- [11] P. Sijtsma. "CLEAN based on spatial source coherence." Int. J. Aeroacoustics, 6, 357–374, 2007.
- [12] R.P. Dougherty and G. Podboy. "Improved Phased Array Imaging of a Model Jet." American Institute of Aeronautics and Astronautics Paper 2009-3186. 2009.